



Published in final edited form as:

J Biophotonics. 2018 May ; 11(5): e201700238. doi:10.1002/jbio.201700238.

Evaluating the effects of maternal alcohol consumption on murine fetal brain vasculature using optical coherence tomography

Raksha Raghunathan^{#1}, Chen Wu^{#1}, Manmohan Singh¹, Chih-Hao Liu¹, Rajesh C. Miranda², and Kirill V. Larin^{1,3,4,*}

¹Department of Biomedical Engineering, University of Houston, Houston, Texas

²Department of Neuroscience and Experimental Therapeutics, Texas A&M Health Science Center, College of Medicine, College Station, Texas

³Interdisciplinary Laboratory of Biophotonics, Tomsk State University, Tomsk, Russia

⁴Molecular Physiology and Biophysics, Baylor College of Medicine, Houston, Texas

These authors contributed equally to this work.

Abstract

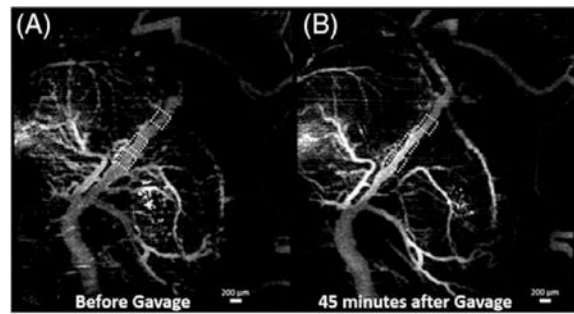
Prenatal alcohol exposure (PAE) can result in a range of anomalies including brain and behavioral dysfunctions, collectively termed fetal alcohol spectrum disorder. PAE during the 1st and 2nd trimester is common, and research in animal models has documented significant neural developmental deficits associated with PAE during this period. However, little is known about the immediate effects of PAE on fetal brain vasculature. In this study, we used *in utero* speckle variance optical coherence tomography, a high spatial- and temporal-resolution imaging modality, to evaluate dynamic changes in microvasculature of the 2nd trimester equivalent murine fetal brain, minutes after binge-like maternal alcohol exposure. Acute binge-like PAE resulted in a rapid (<1 hour) and significant decrease ($P < .001$) in vessel diameter as compared to the sham group. The data show that a single binge-like maternal alcohol exposure resulted in swift vasoconstriction in fetal brain vessels during the critical period of neurogenesis.

Graphical Abstract

*Correspondence: Kirill V. Larin, Department of Biomedical Engineering, University of Houston, Houston, TX. klarin@uh.edu.

AUTHOR BIOGRAPHIES

Please see Supporting Information online.



Keywords

brain vasculature; fetal alcohol spectrum disorder; murine fetus; optical coherence tomography; prenatal alcohol exposure

1 | INTRODUCTION

Fetal alcohol spectrum disorders (FASD) refer to the broad spectrum of developmental and behavioral effects caused by alcohol exposure during pregnancy [1]. FASD is a common source of intellectual and other developmental disabilities, with an estimated global prevalence of 22.77 per 1000 births. Regional estimates of FASD prevalence vary from 33.5 per 1000 births in the United States to 113.22 per 1000 births in South Africa [2]. The range of abnormalities associated with FASD depend upon alcohol dose and gestational period of exposure. However, no amount of alcohol is considered safe during pregnancy [1]. Other contributory factors, including smoking and socioeconomic factors, may be associated with an increased severity of effects due to prenatal alcohol exposure (PAE) [3]. Due to the prevalence of unplanned pregnancies [4] and binge patterns of alcohol consumption [5], the risk for inadvertent PAE during early stages of pregnancy, and even into the 2nd trimester, is high [6]. This high-risk period for PAE also encompasses the peak period for neurogenesis, that is, the fetal period when most neurons of the adult brain are born [7]. Significant work has been done to understand the effects of PAE on the fetal brain [8–16], showing that several aspects of neural development are affected, leading to cognitive and behavioral deficits [17, 18]. The microvasculature that develops in the fetal brain during the 1st and 2nd trimesters supports nutritional needs [19], provides endocrine control of fetal growth [20], and promotes neural development [21]. Although several studies have documented changes in blood flow in the fetal brain after maternal alcohol consumption [22, 23], acute changes in the vasculature of the fetal brain are not well understood or documented.

Traditionally, histological sectioning was used to evaluate embryonic brain development. In addition to being invasive and time consuming, the need to fix tissue can significantly alter the gross morphology of the tissue [24, 25]. Several noninvasive imaging modalities have been developed to study murine embryonic development including confocal microscopy, ultrasound biomicroscopy, micromagnetic resonance imaging and microcomputed tomography [26]. However, due to trade-offs between resolution and imaging depth, motion artifacts from long acquisition times, external contrast agents, and/or the use of ionizing radiation, these methods are unsuitable for imaging live embryos *in utero*. On the other

hand, optical coherence tomography (OCT) [27] is a well-developed optical imaging modality that has been successfully used for imaging small animal embryos over the past decade. Due to its ability to provide cross-sectional images of specimens noninvasively with high spatial and temporal resolution, OCT has been preferred over the other aforementioned imaging modalities for imaging embryonic development. The readers are referred to review papers on the use of OCT for embryonic imaging [28, 29]. For example, OCT is capable of imaging blood vessels less than 50 μm in diameter, which other modalities such as ultrasound biomicroscopy are incapable of resolving [30]. We have demonstrated the superior capabilities of OCT for mouse and rat embryonic imaging during normal and abnormal development [31–36].

Many functional extensions of OCT have been developed, including Doppler OCT [37, 38], and speckle variance OCT (SVOCT) [39–41], a subset of angiographic OCT [42], which have extended the capabilities of OCT from simple structural imaging of embryos to imaging microvasculature and measuring blood flow velocities [34, 43, 44]. For example, OCT has been used extensively to measure the effects of prenatal alcohol exposure on avian embryo cardiovascular structure and function [45–48]. In this study, we use SVOCT [49], a type of angiographic OCT, to detect vasculature changes in the 14.5 DPC (days postcoitum) fetal brain, minutes after maternal ethanol consumption of a binge-like bolus. Pregnant mice were administered ethanol via intragastric gavage, and SVOCT measurements were taken before and every 5 minutes after gavage for 45 minutes. In this work, we report that binge-type PAE resulted in a rapid and sustained decrease in vessel diameter compared to a sham group, demonstrating that maternal alcohol consumption can cause drastic changes in the fetal brain vasculature within minutes.

2 | MATERIALS AND METHODS

2.1 | OCT system

A phase-stabilized swept source OCT system (PhS-SSOCT, schematic shown in Figure 1) was used for structural and speckle variance (functional) imaging of the embryonic brains. The PhS-SSOCT system was composed of a broadband swept source laser source (Santec Corporation, Komaki, Japan) with a central wavelength of 1310 nm, scan range of 150 nm, scan rate of 30 kHz, output power of 39 mW and axial resolution of 11 μm in air. The interference pattern was recorded by a balanced photodetector and digitized by a high-speed analog-to-digital converter. After resampling the raw interference pattern into linear k-space, a fast Fourier transform was performed on the fringe to obtain a 1D depth profile, called an A-scan. Using a scanning galvanometer-mounted mirror, a 2D cross-sectional image was constructed, called a B-scan. More information on the system can be found in our previous work [50].

2.2 | Animal manipulations

All procedures were performed under an approved protocol by the University of Houston Institutional Animal Care and Use Committee. Pregnant CD-1 mice (Charles River Laboratories, Inc. Wilmington, MA) were obtained by timed overnight matings. The presence of a vaginal plug was considered 0.5 DPC. On 14.5 DPC, corresponding to the

transition between the 1st and 2nd trimester equivalent period of brain development [7, 51], pregnant female mice were anesthetized by inhalation of isoflurane (induction: 1%–3%), weighed and placed on a heated platform at 37°C for the duration of the imaging procedure. The depth of maternal anesthesia was maintained with a continuous flow of isoflurane (maintenance: 1.5%–2%) until the last measurement. Abdominal hair was removed, and a small incision was made to expose the uterine horn for imaging. The embryo selected for imaging was stabilized using forceps to minimize bulk motion, and OCT imaging of the embryonic brain was performed through the uterine wall. Imaging parameters and processing are discussed in the next section. After initial pre-alcohol measurements, the pregnant mouse was given a binge-like bolus of 16.6% ethanol (ACS grade, Sigma-Aldrich, St. Louis, MO, USA and CAS# 64–17-5), at a volume of 3 g/kg in water, by intragastric gavage (26G × 38, 1.5 mm tip, Gavageneedle.com). Subsequent measurements were made every 5 minutes for a 45 minutes period after gavage. For the sham group, an equivalent volume of water, instead of ethanol, was given through intra-gastric gavage, and the same imaging procedure was followed. After all measurements were completed, the animal was euthanized by an overdose of isoflurane (overdose: 5%) followed by cervical dislocation. A total of 6 animals were used for this study, randomly selected as 3 in the ethanol group (mean weight: 50.3 ± 7.5 g) and 3 in the sham group (mean weight: 48.7 ± 9.0 g). The animals were housed in an AAALAC-accredited animal facility at the University of Houston on a 12 hours light/dark cycle with ad libitum access to food and water.

2.3 | SVOCT imaging, data processing and quantifications

SVOCT images were obtained by using an algorithm described in our previous work [49]. The OCT probe beam was scanned over an area of 4.4 × 4.7 mm. The 3D SVOCT images consisted of 600 B-scans per volume, and each B-scan had 600 A-scans. Five B-scans were recorded at each spatial position for SVOCT imaging. The time for each B-scan was 20 ms, and the total acquisition time was 84 seconds including the galvanometer flyback time between B-scans. To visualize the vasculature by SVOCT, the variance of the OCT intensity signal at each pixel between successive B-scans recorded at the same spatial position was calculated. Figure 2A shows the 3D OCT structural image with the SVOCT data overlaid. To demonstrate the difference between blood vessels in the uterus and those in the fetal brain, a cross-section from the combined SVOCT and OCT structural image is shown in Figure 2B. The cross-sectional plane in Figure 2B corresponds to the yellow line in Figure 2A. From this cross-section, it is apparent that the vessel on the far right of Figure 2A, which is represented by the dotted yellow circle, is located in the uterine wall, whereas the blood vessels in the left portion of the image are located in the fetal brain. Since the vessels on the uterus and the embryonic brain can be distinguished easily, we ensured that all vessel quantifications reported in this study were from the vessels in the fetal brain. The vessels imaged in this study were dorsal vessels on the embryonic brain at a depth of approximately 100 μm from the surface of the uterus.

An average intensity projection along the axial dimension of the 3D SVOCT image provided an *en face* view of the vasculature in the embryonic brain and the uterus of the mother. Although bulk motion from maternal respiration and heartbeat was minimized during acquisition with forceps, all bulk motion could not be fully prevented. Hence, bulk motion

artifact correction was performed during SVOCT postprocessing. The average SVOCT intensities at each B-scan position were plotted to identify the B-scans that were affected by bulk motion. A threshold value was selected, and any B-scan with an average SVOCT value greater than this threshold was replaced with the previous SVOCT B-scan, assuming that there was sufficiently high-spatial sampling between adjacent B-scans [52]. The 2D average intensity projection was further de-noised in Amira (EFI Co., Portland, OR) using a Gaussian smoothing and a noise-reduction median filter to improve image quality.

A hessian filter based approach was used to enhance the contrast and connectivity of the blood vessels in the 2D projection (Hessian based Frangi Vesselness filter, Dirk-Jan Kroon, MathWorks File Exchange, Mathworks, Natick, MA, USA). The output was thresholded by a binary mask and the vessel diameter was calculated using Matlab (Math-works, Naticka, MA, USA). A nonparametric Friedman test of differences was conducted on each sample to assess statistical significance of the changes in vessel diameter over time. A 2-sided Mann–Whitney *U* test was performed to evaluate if there was a statistical significance in the percentage change of vessel diameter between the 2 treatment groups at 45 minutes after gavage.

3 | RESULTS

Results from 1 embryo each from the sham and alcohol groups are presented in Figures 3 and 4, respectively, followed by the data from 3 embryos from 3 mothers, each from the sham and ethanol groups in Figure 5. Changes in vessel diameter at different positions of the blood vessels were quantified to ensure consistency in results. The data are presented as percentage change in vessel diameter at every time point after gavage with the diameter before gavage as the reference.

Figure 3 depicts results from 1 embryo from the sham group. Figures 3A,B are maximum intensity projections (MIP) of the SVOCT images obtained before and 45 minutes after gavage with water, respectively. Figure 3C plots the percentage change in vessel diameter every 5 minutes for 45 minutes after gavage. As seen from Figure 3, there is no noticeable change in vessel diameter over time after gavage with water. The mean of the median values for each time point of the percentage change in vessel diameter was $3.0\% \pm 1.9\%$.

Figure 4 shows results from 1 embryo from the ethanol group. Figures 4A,B are MIPs of the SVOCT images obtained before and 45 minutes after gavage of the binge-like bolus of ethanol to the mother, respectively. Figure 4C plots the percentage change in vessel diameter every 5 minutes for 45 minutes after gavage with the pre-gavage diameter as a reference. As seen from Figure 4, there is a large decrease in vessel diameter over time after administration of ethanol. At 5 minutes after the alcohol was given, the intra-measurement median percentage decrease in vessel diameter was 2.0%, which increased to 31.9% 45 minutes after the alcohol was given to the mother.

The bright white spots seen on the SVOCT images in Figures 3 and 4 are due to dehydration of the uterine tissue. The uterus was not hydrated with saline for the entire imaging period

due to the possibility of saline interfering with the effects of ethanol. The samples from the sham group were also not hydrated for the entire imaging period to maintain consistency.

Table 1 summarizes the results of the Friedman ANOVA performed on all samples. All samples from the ethanol group showed statistically significant changes in diameter over time, whereas all the samples from the sham group showed no statistically significant changes.

Figure 5 is a summary of the results from all samples ($n = 9$ measurements for each group) at 45 minutes post-gavage. The box represents the interquartile range, the whiskers are the SD and the inscribed hollow squares represent the mean of the data distribution. The Mann–Whitney U test showed that the ethanol group had a highly statistically significant decrease in diameter as compared to the sham group ($n_1 = n_2 = 9$, $U = 0.0004$, $P < .001$).

4 | DISCUSSION

The mid-first trimester through the end of second trimester equivalent period of mouse gestation encompasses the peak period of fetal neurogenesis [7] and angiogenesis [19]. Consequently, brain development during this period of gestation is particularly vulnerable to alcohol. Hence, vasculature changes caused by PAE could have a drastic influence on subsequent brain development. We utilized SVOCT to study acute vascular changes in the fetal brain *in utero* after maternal ethanol exposure. Our results show a drastic decrease in vessel diameter 45 minutes after maternal ethanol consumption. In contrast, the sham animals showed only minimal and nonsignificant changes in vessel diameter over time. These results are from a single binge-like exposure to ethanol at the transition between the first and second trimester equivalent periods (14.5 DPC).

In both sham (Figure 3B vs Figure 3A) and binge-alcohol treated fetuses (Figure 4B vs Figure 4A), we observed a disappearance of smaller tributaries emanating from the larger visualized vessels. This gradual loss over time, which was observed in both control and alcohol exposed fetuses, was perhaps due to effects of prolonged isoflurane anesthesia or due to partial occlusion of uterine vasculature during the process of exteriorization and immobilization of the uterine horn. Previous studies have shown that the maternal heart rate was not significantly lowered by isoflurane anesthesia, and that ethanol itself did not alter maternal heart rate or blood flow, suggesting that the interaction between anesthesia and ethanol is minimal [22]. Consequently, the measured reductions in fetal cranial vessel diameter were likely specifically due to acute maternal alcohol exposure. One other factor that could possibly influence the vessel diameter quantifications is the change in optical properties due to the dehydration of the uterus that was depicted in the Figures 3 and 4. However, since dehydration was observed in both the ethanol and sham group, and all our measurements were made on fetal brain vasculature rather than uterine vasculature, we can safely assume that the influence of optical properties on our quantification was negligible.

In this study, ethanol was given at a volume of 3 g/kg to the mother via intragastric gavage. As mentioned earlier, the dose was chosen as previous studies have shown that this dose resulted in a mean peak BAC of 117 mg/dL, representing binge-like intoxication readily

achieved in non-alcoholic human populations [22]. This level of BAC was achieved when 95% ethanol was used. In this work, we used approximately 17% ethanol, as CD-1 mice were used instead of the C57BL/6 strain, which are known to have a higher tolerance toward alcohol. Seeing such drastic effects at such low-concentrations stresses the need for future studies to assess the effects of different concentrations of ethanol at similar doses. However, recent work has shown that even low doses of prenatal alcohol exposure can have noticeable effects [53]. We also notice from Figures 3 and 4 that the larger region of the central blood vessel did not decrease in diameter over time. We hypothesize that this might be a dose-dependent response. Thus, it will also be important for future studies to assess the dose-response relationship between maternal alcohol exposure and fetal brain vascular perfusion. It is also important to determine if the alcohol-induced changes in fetal vasculature persist beyond the period of exposure or are reversed. In a previous study, effects of maternal ethanol on fetal cerebrovascular blood flow were shown to persist for at least 24 hours, demonstrating that the effects of ethanol are persistent beyond the 45 minutes shown in this work [22]. It will also be important in future studies to ascertain if changes in fetal and uterine blood flow are correlated.

Previous studies using ultrasound imaging have shown that maternal binge-alcohol exposure at earlier developmental time points such as 12.5 DPC resulted in an apparent decrease in cardiac stroke volume through fetal cranial arteries as measured by velocity time integral after a single binge-like exposure and also following subsequent repeated daily binge-like exposures [22]. Although our study clearly shows an immediate reduction in the fetal cranial vessel diameter following maternal ethanol exposure at 14.5 DPC, the relationship between vasoconstriction and reduction in cardiac stroke output through fetal cranial arteries remains to be determined. Moreover, other studies have shown that the effects of PAE on fetal development are influenced by the developmental stage at which maternal exposure occurs [54–56]. The mid-first trimester through the second trimester equivalent period is a critical period for fetal neurogenesis [7], angiogenesis and vasculogenesis [19]. Hence, the vasoconstriction seen in this study could have permanent detrimental effects on fetal brain development, which could lead to lifelong physical and mental disabilities. We have already shown distinct morphological changes in the murine fetal brain *ex vivo* after repeated binge-like exposures to alcohol using OCT [12]. Future studies will also need to determine the impact of fetal developmental stage and brain maturation on the cranial vascular effects of PAE.

One important limitation of SVOCT is the inability to perform quantitative analysis of blood flow. Furthermore, studies using Doppler OCT will enable us to evaluate changes in flow rate and correlate them with changes in vasculature. Doppler OCT will also provide the direction of blood flow that will potentially help us in evaluating the difference, if any, between how maternal ethanol consumption affects flow and morphological changes in the arteries vs veins. Flow rate quantifications will also be used to calculate other indices such as velocity time integral, acceleration, and Pourcelot resistive index, which in turn can be used to assess cardiac output, cardiac stroke volume and vascular resistance, respectively.

5 | CONCLUSION

This work has evaluated rapid vasculature changes in the murine fetal brain caused by acute, binge-like maternal ethanol consumption using SVOCT, a functional extension of OCT. The results showed a prominent decrease in fetal vessel diameter that emerged in the first 10 minutes and persisted for 45 minutes after maternal alcohol consumption, which was not present in the sham group, demonstrating the possibility of ethanol acting as a vasoconstrictor on the fetal brain.

Supplementary Material

Refer to Web version on PubMed Central for supplementary material.

ACKNOWLEDGMENTS

The authors would like to thank Ms. Jennifer Nguyen at the University of Houston for technical assistance. This work was supported by grants from National Institutes of Health grants R01HL120140 and R01HD086765.

Funding information

National Institutes of Health, Grant/Award numbers: R01HL120140, R01HD086765

REFERENCES

- [1]. Williams JF, Smith VC, Pediatrics 2015, 136, e1395. [PubMed: 26482673]
- [2]. Roozen S, Peters GJ, Kok G, Townend D, Nijhuis J, Curfs L, Alcohol. Clin. Exp. Res 2016, 40, 18. [PubMed: 26727519]
- [3]. Balaraman S, Schafer JJ, Tseng AM, Wertelecki W, Yevtushok L, Zymak-Zakutnya N, Chambers CD, Miranda RC, PLoS ONE 2016, 11, e0165081. [PubMed: 27828986]
- [4]. Finer LB, ' N. Engl. J. Med. 2016, 374, 843–852. [PubMed: 26962904]
- [5]. Fillmore MT, Jude R, Am. J. Addict 2011, 20, 468. [PubMed: 21838847]
- [6]. SAMHSA NSDUH Report. Substance Abuse and Mental Health Services Administration, Office of Applied Studies, Rockville, MD 2013.
- [7]. Workman AD, Charvet CJ, Clancy B, Darlington RB, Finlay BL, J. Neurosci 2013, 33, 7368. [PubMed: 23616543]
- [8]. Camarillo C, Miranda RC, Gene Expr. 2008, 14, 159. [PubMed: 18590052]
- [9]. Santillano DR, Kumar LS, Prock TL, Camarillo C, Tingling JD, Miranda RC, BMC Neurosci. 2005, 6, 59. [PubMed: 16159388]
- [10]. Vangipuram SD, Grever WE, Parker GC, Lyman WD, Alcohol. Clin. Exp. Res 2008, 32, 339. [PubMed: 18162078]
- [11]. Bearer CF, Neurotoxicology 2001, 22, 625. [PubMed: 11770884]
- [12]. Sudheendran N, Bake S, Miranda RC, Larin KV, J. Biomed. Opt 2013, 18, 20506. [PubMed: 23386196]
- [13]. Lebel C, Roussotte F, Sowell ER, Neuropsychol. Rev 2011, 21, 102. [PubMed: 21369875]
- [14]. Guerri C, Bazinet A, Riley EP, Alcohol Alcohol 2009, 44, 108. [PubMed: 19147799]
- [15]. Mattson SN, Riley EP, Alcohol. Clin. Exp. Res 1998, 22, 279. [PubMed: 9581631]
- [16]. Roebuck TM, Mattson SN, Riley EP, Alcohol. Clin. Exp. Res 1998, 22, 339. [PubMed: 9581638]
- [17]. Carta M, Mameli M, Valenzuela CF, J. Neurosci 2006, 26, 1906. [PubMed: 16481422]
- [18]. West JR, Parnell SE, Chen WJ, Cudd TA, Alcohol. Clin. Exp. Res 2001, 25, 1051. [PubMed: 11505032]
- [19]. Norman MG, O'Kusky JR, J. Neuropathol. Exp. Neurol 1986, 45, 222. [PubMed: 3958756]

- [20]. Fowden AL, Forhead AJ, Horm. Res. Paediatr 2009, 72, 257.
- [21]. Tam SJ, Watts RJ, Annu. Rev. Neurosci 2010, 33, 379. [PubMed: 20367445]
- [22]. Bake S, Tingling JD, Miranda RC, Alcohol. Clin. Exp. Res 2012, 36, 748. [PubMed: 22141380]
- [23]. Parnell SE, Ramadoss J, Delp MD, Ramsey MW, Chen W-JA, West JR, Cudd TA, Exp. Physiol 2007, 92, 933. [PubMed: 17526556]
- [24]. Sharpe J, Ahlgren U, Perry P, Hill B, Ross A, Hecksher-Sorensen J, Baldock R, Davidson D, Science 2002, 296, 541. [PubMed: 11964482]
- [25]. Walls JR, Coultas L, Rossant J, Henkelman RM, PLoS ONE 2008, 3, e2853. [PubMed: 18682734]
- [26]. Dickinson ME, Dev. Dyn 2006, 235, 2386. [PubMed: 16871621]
- [27]. Huang D, Swanson EA, Lin CP, Schuman JS, Stinson WG, Chang W, Hee MR, Flotte T, Gregory K, Puliafito CA, et al., Science 1991, 254, 1178. [PubMed: 1957169]
- [28]. Raghunathan R, Singh M, Dickinson ME, Larin KV, J. Biomed. Opt 2016, 21, 050902.
- [29]. Men J, Huang Y, Solanki J, Zeng X, Alex A, Jerwick J, Zhang Z, Tanzi RE, Li A, Zhou C, IEEE J. Sel. Top. Quantum Electron 2016, 22, 120.
- [30]. Mariampillai A, Leung MK, Jarvi M, Standish BA, Lee K, Wilson BC, Vitkin A, Yang VX, Opt. Lett 2010, 35, 1257. [PubMed: 20410985]
- [31]. Wang S, Garcia MD, Lopez AL, 3rd. , Overbeek PA , Larin KV , Larina IV , Biomed. Opt. Express 2017, 8, 407. [PubMed: 28101427]
- [32]. Wu C, Sudheendran N, Singh M, Larina IV, Dickinson ME, Larin KV, J. Biomed. Opt 2016, 21, 026002.
- [33]. Singh M, Raghunathan R, Piazza V, Davis-Loiacono AM, Cable A, Vedakkan TJ, Janecek T, Frazier MV, Nair A, Wu C, Larina IV, Dickinson ME, Larin KV, Biomed. Opt. Express 2016, 7, 2295. [PubMed: 27375945]
- [34]. Wang S, Singh M, Lopez AL, 3rd. , Wu C, Raghunathan R, Schill A, Li J, Larin KV, Larina IV, Opt. Lett 2015, 40, 4791. [PubMed: 26469621]
- [35]. Larina IV, Syed SH, Sudheendran N, Overbeek PA, Dickinson ME, Larin KV, J. Biomed. Opt 2012, 17, 081410. [PubMed: 23224171]
- [36]. Larina IV, Sudheendran N, Ghosn M, Jiang J, Cable A, Larin KV, Dickinson ME, J. Biomed. Opt 2008, 13, 060506. [PubMed: 19123647]
- [37]. Chen Z, Milner TE, Srinivas S, Wang X, Malekafzali A, van Gemert MJ, Nelson JS, Opt. Lett 1997, 22, 1119. [PubMed: 18185770]
- [38]. Izatt JA, Kulkarni MD, Yazdanfar S, Barton JK, Welch AJ, Opt. Lett 1997, 22, 1439. [PubMed: 18188263]
- [39]. Barton JK, Stromski S, Opt. Express 2005, 13, 5234. [PubMed: 19498514]
- [40]. Mahmud MS, Cadotte DW, Vuong B, Sun C, Luk TW, Mariampillai A, Yang VX, J. Biomed. Opt 2013, 18, 50901. [PubMed: 23616094]
- [41]. Mariampillai A, Standish BA, Moriyama EH, Khurana M, Munce NR, Leung MK, Jiang J, Cable A, Wilson BC, Vitkin IA, Yang VX, Opt. Lett 2008, 33, 1530. [PubMed: 18594688]
- [42]. Zhang A, Zhang Q, Chen CL, Wang RK, J. Biomed. Opt 2015, 20, 100901. [PubMed: 26473588]
- [43]. Larina IV, Ivers S, Syed S, Dickinson ME, Larin KV, Opt. Lett 2009, 34, 986. [PubMed: 19340193]
- [44]. Larina IV, Furushima K, Dickinson ME, Behringer RR, Larin KV, J. Biomed. Opt 2009, 14, 050506. [PubMed: 19895102]
- [45]. Karunamuni G, Gu S, Doughman YQ, Peterson LM, Mai K, McHale Q, Jenkins MW, Linask KK, Rollins AM, Watanabe M, Am. J. Physiol. Heart Circ. Physiol 2014, 306, H414. [PubMed: 24271490]
- [46]. Karunamuni G, Gu S, Doughman YQ, Noonan AI, Rollins AM, Jenkins MW, Watanabe M, Dev. Dyn 2015, 244, 607. [PubMed: 25546089]
- [47]. Karunamuni GH, Ma P, Gu S, Rollins AM, Jenkins MW, Watanabe M, Birth Defects Res. C Embryo Today 2014, 102, 227. [PubMed: 25220155]

- [48]. Peterson LM, Gu S, Karunamuni G, Jenkins MW, Watanabe M, Rollins AM, Biomed. Opt. Express 2017, 8, 1823. [PubMed: 28663868]
- [49]. Sudheendran N, Syed SH, Dickinson ME, Larina IV, Larin KV, Laser Phys. Lett 2011, 8, 247.
- [50]. Manapuram R, Manne V, Larin K, Laser Phys. 2008, 18, 1080.
- [51]. Patten AR, Fontaine CJ, Christie BR, Front. Pediatr 2014, 2, 93. [PubMed: 25232537]
- [52]. Poole KM, McCormack DR, Patil CA, Duvall CL, Skala MC, Biomed. Opt. Express 2014, 5, 4118. [PubMed: 25574425]
- [53]. Muggli E, Matthews H, Penington A, Claes P, O'Leary C, Forster D, Donath S, Anderson PJ, Lewis S, Nagle C, Craig JM, White SM, Elliott EJ, Halliday J, JAMA Pediatr. 2017, 171, 771. [PubMed: 28586842]
- [54]. Ji RP, Phoon CK, Aristizabal O, McGrath KE, Palis J, Turnbull DH, Circ. Res 2003, 92, 133. [PubMed: 12574139]
- [55]. Daft PA, Johnston MC, Sulik KK, Teratology 1986, 33, 93. [PubMed: 3738814]
- [56]. Serrano M, Han M, Brinez P, Linask KK, Am. J. Obstet. Gynecol 2010, 203, 75e77.

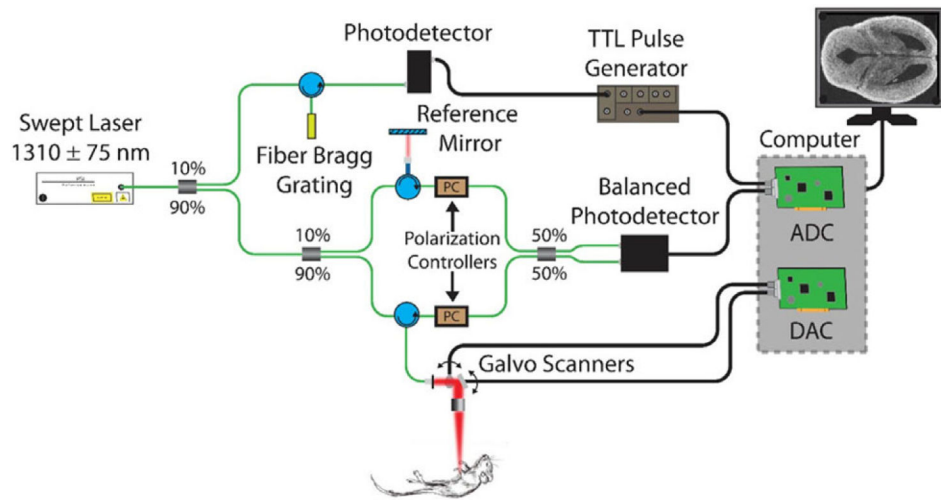


FIGURE 1. OCT system schematic. Analog to digital converter (ADC) and digital to analog converter (DAC)

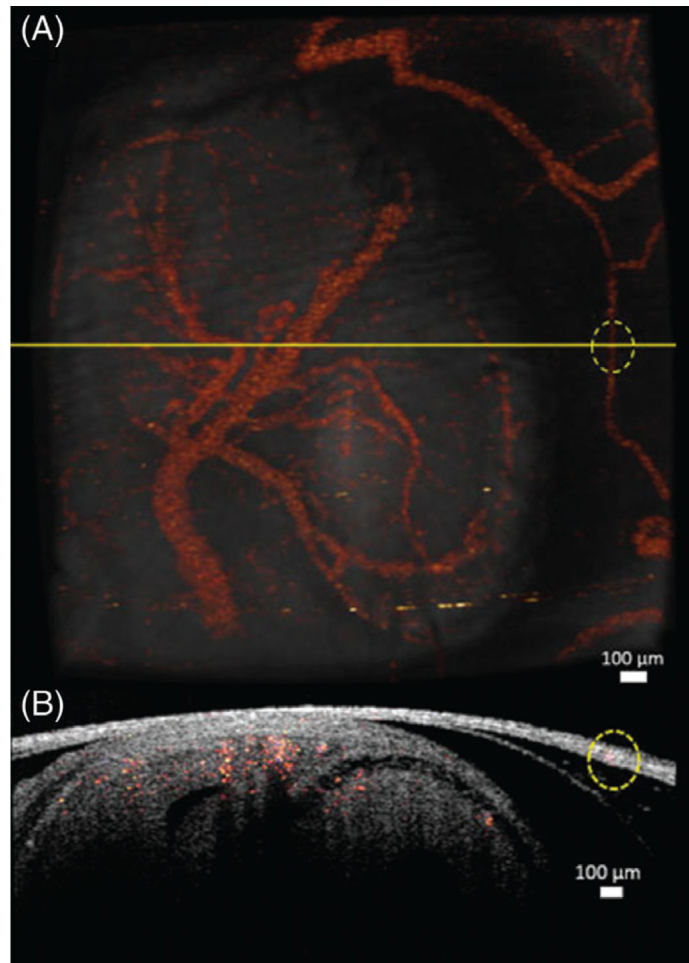


FIGURE 2. (A) 3D structural OCT image overlapped with the 3D SVOCT image. (B) 2D cross-section depicted by the yellow line in (A). The circled region indicates a blood vessel in the uterus

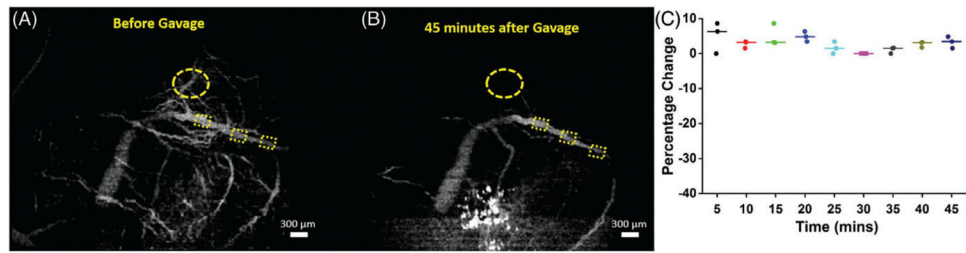


FIGURE 3.

SVOCT images and diameter change of 1 sample from the sham group. (A) MIP of the SVOCT image before intragastric gavage. The dotted squares depict the positions where the diameter was quantified. (B) MIP of the SVOCT image 45 minutes after administration of water by gavage. (C) Percentage change in vessel diameter after administration of water by gavage, every 5 minutes for 45 minutes with the pre-gavage diameter as the reference. The line depicts the interquartile median, and the raw data are plotted alongside. The bright white spots seen on the SVOCT images are due to dehydration of the uterus tissue. The dotted circle shows the gradual disappearance of smaller tributaries

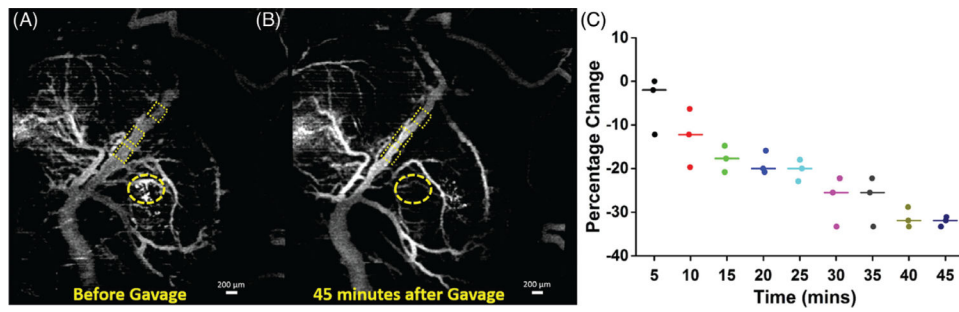


FIGURE 4.

SVOCT images and diameter change of 1 sample from the alcohol group. (A) MIP of the SVOCT image before administration of alcohol by intragastric gavage. The dotted squares depict the positions where the diameter was quantified. (B) MIP of the SVOCT image 45 minutes after administration of alcohol to the mother by gavage. (C) Percentage change in vessel diameter after administration of ethanol by gavage, every 5 minutes for 45 minutes with the pre-gavage diameter as the reference. The line depicts the interposition median, and the raw data are plotted alongside. The bright white spots seen on the SVOCT images are due to dehydration of the uterus tissue. The dotted circle shows the gradual disappearance of smaller tributaries

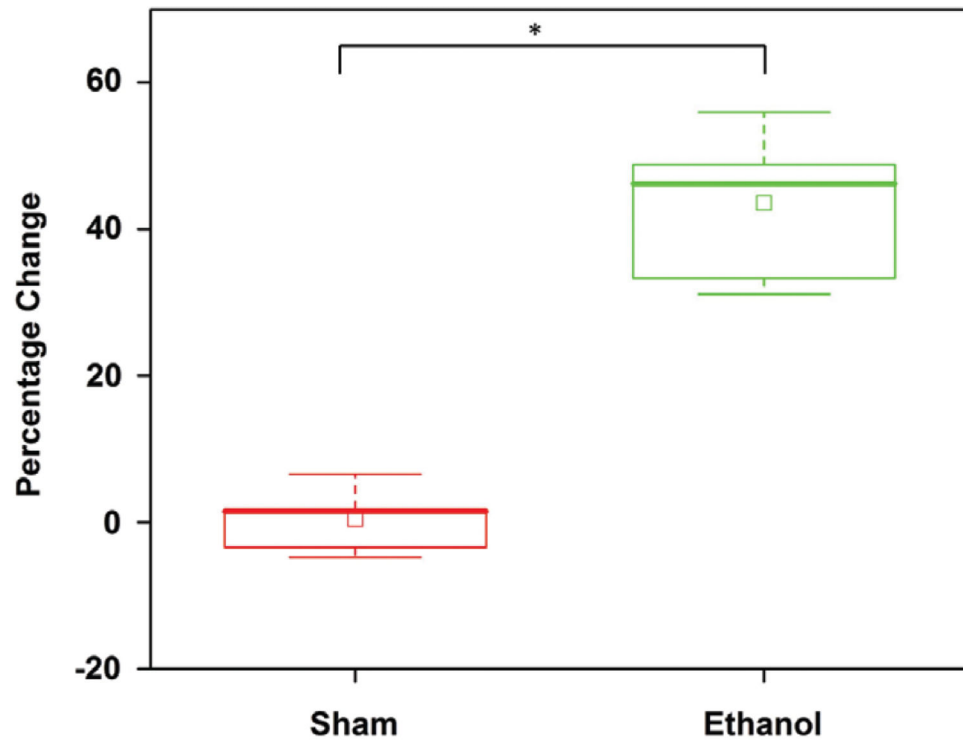


FIGURE 5. Percentage change 45 minutes after administration of (sham) water and ethanol by intragastric gavage. The box is the interquartile range, the whiskers are the outliers, the inscribed squares are the mean and the asterisk indicates $P < .001$ by a 2-sided Mann-Whitney U test

Summary of the Friedman ANOVA results performed on all samples. The degrees of freedom for all tests were 8

TABLE 1

| | Sham group | | | Ethanol group | | |
|----------------|------------|------------|------------|---------------|------------|------------|
| | Sample 1 | Sample 2 | Sample 3 | Sample 1 | Sample 2 | Sample 3 |
| χ^2 value | 12.31 | 6.53 | 11.26 | 22.37 | 23.46 | 16.44 |
| Significance | $P = .137$ | $P = .587$ | $P = .187$ | $P = .004$ | $P = .003$ | $P = .036$ |